

Right-handed sneutrino dark matter and big-bang nucleosynthesis

Koji Ishiwata^(a), Masahiro Kawasaki^(b,c), Kazunori Kohri^(a),
and Takeo Moroi^(a,c)

^a*Department of Physics, Tohoku University, Sendai 980-8578, Japan*

^b*Institute for Cosmic Ray Research, University of Tokyo, Kashiwa 277-8582, Japan*

^c*Institute for the Physics and Mathematics of the Universe, University of Tokyo,
Kashiwa 277-8568, Japan*

Abstract

We study the light-element abundances in supersymmetric model where the right-handed sneutrino is the lightest superparticle (LSP), assuming that the neutrino masses are purely Dirac-type. In such a scenario, the lightest superparticle in the minimal supersymmetric standard model sector (which we call MSSM-LSP) becomes long-lived, and thermal relic MSSM-LSP may decay after the big-bang nucleosynthesis starts. We calculate the light-element abundances including non-standard nuclear reactions induced by the MSSM-LSP decay, and derive constraints on the scenario of right-handed sneutrino LSP.

With the precise astrophysical observations, it is now widely believed that about 23% of the energy density of the present universe is due to dark matter (DM) [1]. The existence of dark matter, however, raises a serious question to particle physics because there is no viable candidate for dark matter in the particle content of the standard model. To solve this problem, many dark-matter models have been proposed so far.

In constructing dark-matter model, it is important to understand how dark matter was produced in the early universe. In many cases, the thermal freeze-out mechanism is adopted to produce dark matter particle in the early universe; then, dark matter particle, which is in thermal bath when the cosmic temperature is higher than its mass, freezes out from the thermal bath when the cosmic temperature becomes low.

However, the freeze-out scenario is not the only possibility to produce dark matter particle in the early universe. Even if the dark matter particle is very weakly interacting so that it is never thermalized, it can be produced by the decay and scattering of particles in thermal bath. In particular, if the interaction of dark matter is dominated by renormalizable ones, dark-matter production is most effective when the temperature is comparable to the mass of parent particle which produces dark matter via the decay or scattering. Thus, if the reheating temperature after inflation is higher than the mass of parent particle, the relic density of the dark matter becomes insensitive to the cosmic evolution in the early stage.

Such a scenario was originally proposed in [2], where the right-handed sneutrino $\tilde{\nu}_R$ in supersymmetric model is shown to be a viable candidate for dark matter. In [2], it was also shown that, if $\tilde{\nu}_R$ -DM is dominantly produced from the decay and scattering of superparticles in thermal bath, the primordial abundance of $\tilde{\nu}_R$ is determined when the cosmic temperature is comparable to the masses of superparticles. Then, recently, more general discussion of such a scenario has been given in [3], where a variety of candidates for such very weakly-interacting dark-matter particles have been also considered.

If a very weakly interacting particle is dark matter, it is often the case that a long-lived particle (with lifetime longer than ~ 1 sec) may show up, which may spoil the success of the standard big-bang nucleosynthesis [4, 5, 2, 6, 3]. This is indeed the case where the right-handed sneutrino is the lightest superparticle (LSP) and is dark matter. If a right-handed sneutrino is the LSP, the lightest superparticle in the minimal supersymmetric standard model (MSSM) sector (which we call MSSM-LSP) decays into $\tilde{\nu}_R$ (and R -even particles) via very small neutrino Yukawa interaction. Then, decay of the MSSM-LSP after the big-bang nucleosynthesis (BBN) epoch may affect the light-element abundances. Thus, it is important to check the BBN constraints on the scenario.

In this letter, we consider the case where a right-handed sneutrino is the LSP, assuming Dirac-type neutrino masses [2].^{#1} We study the light-element abundances in such a case in detail, and derive BBN constraints on the mass and lifetime of the MSSM-LSP. We also comment on the implication of the sneutrino LSP scenario on the ${}^7\text{Li}$ overproduction problem.

First, we discuss the model framework that we consider in this letter. The superpotential

^{#1}For related topics, see also [7].

is written as

$$W = W_{\text{MSSM}} + y_\nu \hat{L} \hat{H}_u \hat{\nu}_R^c, \quad (1)$$

where W_{MSSM} is the superpotential of the MSSM, $\hat{L} = (\hat{\nu}_L, \hat{e}_L)$ and $\hat{H}_u = (\hat{H}_u^+, \hat{H}_u^0)$ are left-handed lepton doublet and up-type Higgs doublet, respectively. (In this letter, “hat” is used for superfields, while “tilde” is for superpartners.) Generation indices are omitted for simplicity. In this model, neutrinos acquire their masses only through Yukawa interactions as $m_\nu = y_\nu \langle H_u^0 \rangle = y_\nu v \sin \beta$, where $v \simeq 174$ GeV is the vacuum expectation value (VEV) of the standard model Higgs field and $\tan \beta = \langle H_u^0 \rangle / \langle H_d^0 \rangle$. Thus, the neutrino Yukawa coupling is determined by the neutrino mass as

$$y_\nu \sin \beta = 3.0 \times 10^{-13} \times \left(\frac{m_\nu^2}{2.8 \times 10^{-3} \text{ eV}^2} \right)^{1/2}. \quad (2)$$

Mass squared differences among neutrinos have already been determined accurately by neutrino oscillation experiments. In particular, the K2K experiment suggests $[\Delta m_\nu^2]_{\text{atom}} \simeq (1.9 - 3.5) \times 10^{-3} \text{ eV}^2$ [8]. In the following discussion, we assume that the spectrum of neutrino masses is hierarchical, hence the largest neutrino Yukawa coupling is of the order of 10^{-13} unless otherwise mentioned; we use $y_\nu = 3.0 \times 10^{-13}$ for our numerical study. (We neglect effects of smaller Yukawa coupling constants.) For our study, it is also necessary to introduce soft supersymmetry (SUSY) breaking terms. Soft SUSY breaking terms relevant to our analysis are

$$\mathcal{L}_{\text{soft}} = -\frac{1}{2}(m_{\tilde{B}} \tilde{B} \tilde{B} + m_{\tilde{W}} \tilde{W} \tilde{W} + \text{h.c.}) - M_{\tilde{L}}^2 \tilde{L}^\dagger \tilde{L} - M_{\tilde{\nu}_R}^2 \tilde{\nu}_R^* \tilde{\nu}_R + (A_\nu \tilde{L} H_u \tilde{\nu}_R^c + \text{h.c.}), \quad (3)$$

where \tilde{B} and \tilde{W} are Bino and Wino, respectively. We parameterize A_ν by using the dimensionless constant a_ν as

$$A_\nu = a_\nu y_\nu M_{\tilde{L}}. \quad (4)$$

Notice that a_ν is a free parameter and, in gravity-mediated SUSY breaking scenario, for example, a_ν is expected to be $O(1)$. The A_ν -term induces the left-right mixing in the sneutrino mass matrix, through which the MSSM-LSP decays in the present case. In the calculation of mass eigenvalues, however, the mixing is negligible because of the smallness of neutrino Yukawa coupling constants, and we obtain

$$m_{\tilde{\nu}_L}^2 \simeq M_{\tilde{L}}^2 + \frac{1}{2} m_Z^2 \cos 2\beta, \quad m_{\tilde{\nu}_R}^2 \simeq M_{\tilde{\nu}_R}^2, \quad (5)$$

where m_Z is the Z boson mass. Here and hereafter, we assume that all the right-handed sneutrinos are degenerate in mass for simplicity. In the numerical study, we take the following model parameters: $m_{\tilde{\nu}_R} = 100$ GeV, $\tan \beta = 30$, and $m_h = 115$ GeV (with m_h being the lightest Higgs boson mass). In addition, the Wino mass is related to the Bino mass using the GUT relation.

In the early universe, right-handed sneutrino is never thermalized because of the weakness of neutrino Yukawa interaction. Although it is decoupled from thermal bath, right-handed sneutrino can be produced in various processes; (i) decay or scattering of MSSM particles in thermal bath, (ii) decay of MSSM-LSP after freeze-out, and (iii) production in very early universe via the decay of exotic particles (like gravitino or inflaton). Thereafter, we donate the contribution of each process as, $\Omega_{\tilde{\nu}_R}^{(\text{Thermal})}$, $\Omega_{\tilde{\nu}_R}^{(\text{F.O.})}$, and $\Omega_{\tilde{\nu}_R}^{(\text{non-MSSM})}$ in order. Primarily, right-handed sneutrino is produced through neutrino Yukawa interaction (and the left-right mixing of sneutrino) dominantly in the following decay processes: $\tilde{H}^0 \rightarrow \tilde{\nu}_R \bar{\nu}$, $\tilde{H}^+ \rightarrow \tilde{\nu}_R l^+$, $\tilde{\nu}_L \rightarrow \tilde{\nu}_R h$, $\tilde{\nu}_L \rightarrow \tilde{\nu}_R Z$, $\tilde{l}_L \rightarrow \tilde{\nu}_R W^-$, $\tilde{B} \rightarrow \tilde{\nu}_R \bar{\nu}$, $\tilde{W}^0 \rightarrow \tilde{\nu}_R \bar{\nu}$, and $\tilde{W}^+ \rightarrow \tilde{\nu}_R l^+$. In the previous work, it was shown that right-handed sneutrino can be adequately produced to become dark matter when the masses of left- and right-handed sneutrino are degenerate at 10 – 20 % with $a_\nu \lesssim 3$, or in a case of larger a_ν without degeneracy [2]. It is also mentioned that enhancement of right-handed sneutrino production is possible with larger neutrino Yukawa coupling if we consider the case where neutrino masses are degenerate. Giving an eye on the thermal bath again, the MSSM-LSP decouples from thermal bath and its number freezes out in the same manner with usual MSSM, while the number of the other MSSM particles is suppressed by Boltzmann factor in this epoch. However, relic MSSM-LSP, which is assumed to be the next-to-the-lightest superparticle (NLSP) in this letter, decays to right-handed sneutrino through neutrino Yukawa coupling in the late time. In this process, the contribution to the abundance is given as

$$\Omega_{\tilde{\nu}_R}^{(\text{F.O.})} = \frac{m_{\tilde{\nu}_R}}{m_{\text{NLSP}}} \Omega_{\text{NLSP}}^{(\text{F.O.})}, \quad (6)$$

where m_{NLSP} is the mass of the NLSP and $\Omega_{\text{NLSP}}^{(\text{F.O.})}$ is the would-be density parameter of the relic NLSP (for the case where it does not decay into $\tilde{\nu}_R$). Lastly, we mention that there might be a possibility that right-handed sneutrino is produced directly from an exotic particle in the very early universe. The abundance of the expected right-handed sneutrino is model-dependent, and we do not discuss further detail of specific model. In this letter, we consider the scenario that right-handed sneutrino produced in these processes becomes dark matter. We do not specify which is dominant process to produce right-handed sneutrino.

If $\tilde{\nu}_R$ is the LSP, it is always the case that the MSSM-LSP becomes long-lived. Because some amount of relic NLSP always exists in the early universe, they may cause serious problem in BBN; if the relic MSSM-LSP decays during or after the BBN epoch, energetic charged and/or colored particles are emitted; they cause the photo- and hadro-dissociation processes of light elements, which may spoil the success of the standard BBN scenario. In the following, we consider three typical candidates for the MSSM-LSP; Bino \tilde{B} , left-handed sneutrino $\tilde{\nu}_L$, and lighter stau $\tilde{\tau}$, and study how the $\tilde{\nu}_R$ -DM scenario is constrained by the BBN.

In the Bino-NLSP case, the Bino dominantly decays as $\tilde{B} \rightarrow \tilde{\nu}_R \bar{\nu}$ (and its CP-conjugated

process) and its decay rate is given by^{#2}

$$\Gamma_{\tilde{B} \rightarrow \tilde{\nu}_R \bar{\nu}} = \frac{\beta_f^2 g_1^2}{64\pi} \left[\frac{A_\nu v}{m_{\tilde{\nu}_L}^2 - m_{\tilde{\nu}_R}^2} \right]^2 m_{\tilde{B}}, \quad (7)$$

where g_1 is the $U(1)_Y$ gauge coupling constant and, for the process $x \rightarrow \tilde{\nu}_R y$, β_f is given by

$$\beta_f^2 = \frac{1}{m_x^4} [m_x^4 - 2(m_{\tilde{\nu}_R}^2 + m_y^2)m_x^2 + (m_{\tilde{\nu}_R}^2 - m_y^2)^2], \quad (8)$$

with m_x and m_y being the masses of the particles x and y , respectively. When $\tilde{\nu}_L$ or $\tilde{\tau}$ is the NLSP, the NLSP decays by emitting weak- or Higgs-boson if kinematically allowed. The decay rates for those processes are given by

$$\Gamma_{\tilde{\nu}_L \rightarrow \tilde{\nu}_R Z} = \frac{\beta_f^3}{32\pi} \left[\frac{m_{\tilde{\nu}_L}^2}{m_{\tilde{\nu}_L}^2 - m_{\tilde{\nu}_R}^2} \right]^2 \frac{A_\nu^2}{m_{\tilde{\nu}_L}}, \quad (9)$$

$$\Gamma_{\tilde{\nu}_L \rightarrow \tilde{\nu}_R h} = \frac{\beta_f}{32\pi} \frac{A_\nu^2}{m_{\tilde{\nu}_L}}, \quad (10)$$

$$\Gamma_{\tilde{\tau} \rightarrow \tilde{\nu}_R W^-} = \frac{\beta_f^3 \sin^2 \theta_{\tilde{\tau}}}{16\pi} \left[\frac{m_{\tilde{\tau}}^2}{m_{\tilde{\nu}_L}^2 - m_{\tilde{\nu}_R}^2} \right]^2 \frac{A_\nu^2}{m_{\tilde{\tau}}}, \quad (11)$$

where $m_{\tilde{\tau}}$ is the stau mass and $\theta_{\tilde{\tau}}$ is the left-right mixing angle of stau. (The lighter stau is given by $\tilde{\tau} = \tilde{\tau}_R \cos \theta_{\tilde{\tau}} + \tilde{\tau}_L \sin \theta_{\tilde{\tau}}$.) If the two-body processes are kinematically blocked, the slepton-NLSP decays into three-body final state as $\tilde{\nu}_L \rightarrow \tilde{\nu}_R f \bar{f}$ and $\tilde{\tau} \rightarrow \tilde{\nu}_R f \bar{f}'$ (with f and f' being standard-model fermions).

Now, we are at the position to discuss the BBN constraints on $\tilde{\nu}_R$ -DM scenario. We start with the case where Bino is NLSP. As we have mentioned, the Bino-NLSP dominantly decays as $\tilde{B} \rightarrow \tilde{\nu}_R \bar{\nu}$. Since $\tilde{\nu}_R$ and ν are (very) weakly interacting particles, the BBN constraints are not so severe if this is the only possible decay mode. However, \tilde{B} may also decay as $\tilde{B} \rightarrow \tilde{\nu}_R \bar{\nu} Z^{(*)}$ and $\tilde{\nu}_R l W^{(*)}$, where $Z^{(*)}$ and $W^{(*)}$ are on-shell or off-shell Z and W bosons (where the “star” is for off-shell particle), respectively, while l is charged lepton. Then, through the decay of $Z^{(*)}$ and $W^{(*)}$, quarks and charged leptons are produced. Even though the branching ratio for such processes are phase-space suppressed, they produce sizable amount of hadrons which may significantly affect the light-element abundances. Thus, in our analysis, effects of those decay modes are taken into account in deriving the BBN constraints. The light-element abundances also depend on the primordial abundance of the NLSP, and we adopt the abundance of Bino in the focus-point (or co-annihilation) region [9]^{#3}

$$Y_{\tilde{B}}^{(\text{focus})} = 9 \times 10^{-13} \times \left(\frac{m_{\tilde{B}}}{100 \text{ GeV}} \right), \quad (12)$$

^{#2}In this letter, we consider the case where the Gaugino-Higgsino mixing is so small that its effect is negligible.

^{#3}If the Bino is the NLSP, its primordial abundance strongly depends on the MSSM parameters. In the

where the yield variable is defined as $Y_x \equiv n_x/s$ with n_x being the number density of particle x and s the entropy density of the universe.

Following the procedure given in [10], we calculate the light-element abundances taking account of the hadro-dissociation, photo-dissociation, and $p \leftrightarrow n$ conversion processes. The energy distribution of the final-state particles are calculated by using the HELAS package [11], and the hadronization processes of colored particles are studied by using the PYTHIA package [12]. In the Bino-NLSP case, high energy neutrino emitted by the Bino decay may scatter off background neutrino and generate energetic e^\pm , which becomes the source of energetic photon [13]. In our analysis, we have taken into account the effects of the photo-dissociation process induced by photon from the neutrino injection. (However, we found that the neutrino-induced processes are less important compared to other processes.) Once theoretical values of the primordial light-element abundances are obtained as functions of the mass and the lifetime of the NLSP, we compare them with the observed values of the primordial abundances. In deriving the constraints on the model, we adopt the following observational constraints:

- D to H ratio [14, 15]:

$$(n_{\text{D}}/n_{\text{H}})_{\text{p}} = (2.82 \pm 0.26) \times 10^{-5}. \quad (13)$$

- ^4He mass fraction [16, 17]:

$$Y_{\text{p}} = 0.2516 \pm 0.0040. \quad (14)$$

- ^3He to D ratio [18, 10]:

$$(n_{^3\text{He}}/n_{\text{D}})_{\text{p}} < 0.83 + 0.27. \quad (15)$$

- ^6Li to ^7Li ratio [19, 20]:^{#4}

$$(n_{^6\text{Li}}/n_{^7\text{Li}})_{\text{p}} < 0.046 + 0.022 + 0.106. \quad (16)$$

- ^7Li to H ratio [22, 20]:

$$\log_{10}(n_{^7\text{Li}}/n_{\text{H}})_{\text{p}} = -9.90 \pm 0.09 + 0.35. \quad (17)$$

so-called bulk region, the abundance is larger, and is approximately given by

$$Y_{\tilde{B}}^{(\text{bulk})} = 4 \times 10^{-12} \times \left(\frac{m_{\tilde{B}}}{100 \text{ GeV}} \right).$$

We have checked that the BBN constraints in such a case are almost the same as the focus-point case. If we adopt the abundance in the bulk region, however, $\Omega_{\tilde{\nu}_R}^{(\text{F.O.})}$ becomes larger than the present dark matter density if $m_{\tilde{\nu}_R} = 100 \text{ GeV}$. Thus we will not consider such a case in the following discussion.

^{#4}Asplund *et al.* reported $n_{^6\text{Li}}/n_{^7\text{Li}} = 0.046 \pm 0.022$. However, their positive detection has not been fully confirmed yet as pointed out in [21]. Therefore, we consider the observed value as an upper bound.

(Here and hereafter the subscript “p” denotes the primordial value inferred by observation.) As shown in (16) and (17), we add positive systematic errors of +0.106 and +0.35 to the observational face-values of $(n_{6\text{Li}}/n_{7\text{Li}})_p$ and $\log_{10}(n_{7\text{Li}}/n_{\text{H}})_p$, respectively. We expect that these systematic errors result from possible depletion in stars through rotational mixing [23] or diffusion [24]. Since both ${}^7\text{Li}$ and ${}^6\text{Li}$ are destroyed by depletion process, their systematic errors are correlated (for more details, see [20]). We note here that the standard BBN is excluded at more than $4\text{-}\sigma$ level if we do not adopt the systematic error on ${}^7\text{Li}$ abundance [25] (so-called ${}^7\text{Li}$ problem). Thus, to derive a conservative constraint, we add these systematic errors. At the end of this letter, we will comment on implications of the $\tilde{\nu}_R$ -DM scenario on the ${}^7\text{Li}$ problem.^{#5}

In Fig. 1, we show the constraint from BBN for the Bino-NLSP case on $m_{\tilde{B}}$ vs. $\tau_{\tilde{B}}$ plane (with $\tau_{\tilde{B}}$ being the lifetime of Bino). The lifetime is related to the fundamental parameters via Eq. (7); in particular, $\tau_{\tilde{B}}$ is proportional to a_ν^{-2} . Taking $m_{\tilde{\nu}_L} = 1.2m_{\tilde{B}}$, we calculate a_ν -parameter. In the figure, un-shaded, lightly shaded, and darkly shaded regions indicate the region with $a_\nu < 1$, $1 < a_\nu < 10$, and $a_\nu > 10$, respectively. One can see that the region with $m_{\tilde{B}} \lesssim 200$ GeV is always allowed. This is because, in such a region, the dominant hadronic decay processes are four-body ones ($\tilde{B} \rightarrow \tilde{\nu}_R \bar{\nu} q \bar{q}$ and $\tilde{\nu}_R l q \bar{q}'$), for which the branching ratio is significantly suppressed by the phase-space factor. On the other hand, when the decay processes $\tilde{B} \rightarrow \tilde{\nu}_R \bar{\nu} Z$ and $\tilde{\nu}_R l W$ are kinematically allowed, those three-body decay processes have sizable branching ratio, resulting in an enhanced production of hadrons. We can see that the lifetime of Bino is constrained to be smaller than $\tau_{\tilde{B}} \lesssim 10^2$ sec in such a parameter region in order not to overproduce deuterium via the hadro-dissociation of ${}^4\text{He}$.

In the figure, we also plot contours of constant density parameters. Once the primordial abundance of the NLSP is fixed, $\Omega_{\tilde{\nu}_R}^{(\text{F.O.})}$ is calculated by using Eq. (6). We show the contour of $\Omega_{\tilde{\nu}_R}^{(\text{F.O.})} = \Omega_c = 0.228$ [1]; the right-hand side of the line is excluded by the overclosure constraint if we adopt the abundance given in Eq. (12). In studying the $\tilde{\nu}_R$ -DM scenario, we should also consider $\tilde{\nu}_R$ from the MSSM particles in the thermal bath. Following [2], we calculate the sneutrino abundance by solving the Boltzmann equation taking account of all the relevant sneutrino production processes. The contour of $\Omega_{\tilde{\nu}_R}^{(\text{Thermal})} = \Omega_c$ is shown in Fig. 1; the a_ν -parameter is determined by using Eq. (7), while the MSSM parameters are taken to be $m_{\tilde{\nu}_L} = 1.2m_{\tilde{B}}$, and $\mu_H = 2m_{\tilde{B}}$ (with μ_H being the SUSY invariant Higgs mass). $\tilde{\nu}_R$ is overproduced below the line of $\Omega_{\tilde{\nu}_R}^{(\text{Thermal})} = \Omega_c$ with the present choice of parameters. One can see that the line is well below the constrained region by BBN. In the present choice of parameters, a relatively large value of a_ν is needed unless the masses of \tilde{B} and $\tilde{\nu}_R$ are degenerate in order to realize $\Omega_{\tilde{\nu}_R}^{(\text{Thermal})} = \Omega_c$. However, notice that the relic abundance of $\tilde{\nu}_R$ depends on various parameters. In particular, $\Omega_{\tilde{\nu}_R}^{(\text{Thermal})}$ becomes larger when the mass difference between $\tilde{\nu}_R$ and $\tilde{\nu}_L$ becomes smaller because the left-right mixing is enhanced. In

^{#5}As we will discuss later in considering the ${}^7\text{Li}$ problem, one may adopt a slightly higher value of D to H ratio, $(n_{\text{D}}/n_{\text{H}})_p = (3.98_{-0.67}^{+0.59}) \times 10^{-5}$ [14], and/or that of ${}^7\text{Li}$ to H ratio, $\log_{10}(n_{7\text{Li}}/n_{\text{H}})_p = -9.63 \pm 0.06$ [26]. We have checked that, even with these observational constraints, the constraints given in Figs. 1 – 3 are almost unchanged (as far as the systematic error in the ${}^7\text{Li}$ abundance is taken into account).

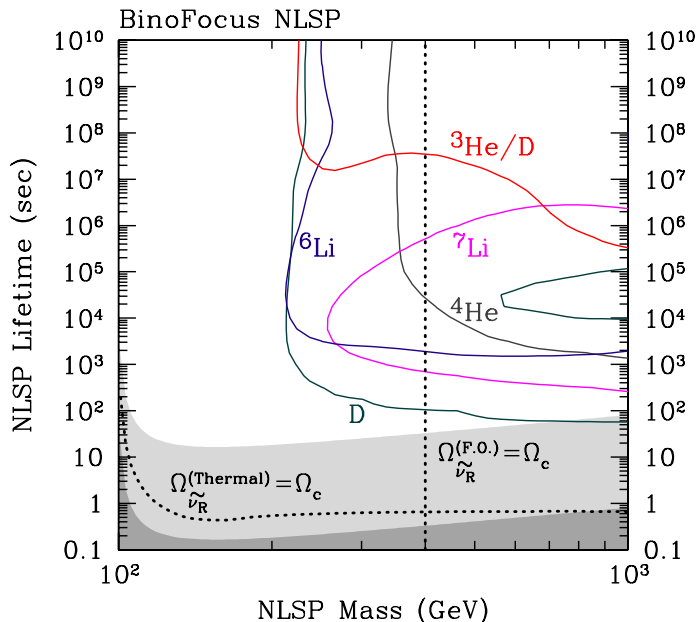


Figure 1: BBN constraints on the Bino-NLSP case are shown on $m_{\tilde{B}}$ vs. $\tau_{\tilde{B}}$ plane. The un-shaded, lightly shaded, and darkly shaded regions are for $a_\nu < 1$, $1 < a_\nu < 10$, and $a_\nu > 10$, respectively. In addition, the contours of $\Omega_{\tilde{\nu}_R}^{(\text{F.O.})} = \Omega_c$ and $\Omega_{\tilde{\nu}_R}^{(\text{Thermal})} = \Omega_c$ are also shown (dotted lines). For the calculation of $\Omega_{\tilde{\nu}_R}^{(\text{Thermal})}$, we take $m_{\tilde{\nu}_R} = 100$ GeV, $m_{\tilde{\nu}_L} = 1.2m_{\tilde{B}}$, $\mu_H = 2m_{\tilde{B}}$, $m_h = 115$ GeV, and $\tan\beta = 30$.

addition, $\Omega_{\tilde{\nu}_R}^{(\text{Thermal})}$ is also enhanced if we use a larger value of the neutrino Yukawa coupling constant; it may happen when we adopt the degenerate neutrino masses. Thus, with other choices of parameters, the required value of a_ν to realize $\Omega_{\tilde{\nu}_R}^{(\text{Thermal})} = \Omega_c$ changes.

Another candidate for the NLSP is the left-handed sneutrino. Such a scenario is attractive in the $\tilde{\nu}_R$ -DM scenario because the $\tilde{\nu}_R$ abundance is enhanced if the masses of $\tilde{\nu}_R$ and $\tilde{\nu}_L$ becomes closer. When $\tilde{\nu}_L$ is the NLSP, its dominant decay process is $\tilde{\nu}_L \rightarrow \tilde{\nu}_R Z^{(*)}$ and $\tilde{\nu}_L \rightarrow \tilde{\nu}_R h^{(*)}$. Thus, colored and/or charged particles are effectively produced via the dominant decay modes. Again, we calculate the light-element abundances taking account of the hadro-dissociation, photo-dissociation, and $p \leftrightarrow n$ conversion processes, and compare the resultant light-element abundances with observational constraints given in (13) – (17). The relic abundance of left-handed sneutrino is approximated as [27]:

$$Y_{\tilde{\nu}_L} \simeq 2 \times 10^{-14} \times \left(\frac{m_{\tilde{\nu}}}{100 \text{ GeV}} \right). \quad (18)$$

The BBN constraints are shown in Fig. 2. We can see that the parameter space is constrained as $\tau_{\tilde{\nu}_L} \lesssim 10^2$ sec (with $\tau_{\tilde{\nu}_L}$ being the lifetime of $\tilde{\nu}_L$) by the deuterium overproduction irrespective of $m_{\tilde{\nu}_L}$. This is due to the fact that, if $\tilde{\nu}_L$ is the NLSP, production of hadrons occurs in the dominant decay processes. This is a large contrast to the Bino-NLSP case.

If $\tilde{\nu}_L$ is the NLSP, its primordial abundance is so small that $\Omega_{\tilde{\nu}_R}^{(\text{F.O.})} < \Omega_c$ as far as

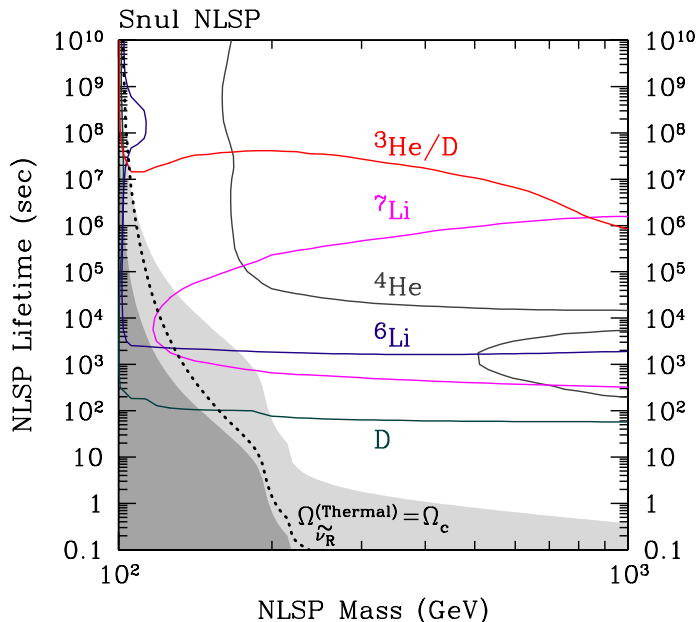


Figure 2: BBN constraints on the $\tilde{\nu}_L$ -NLSP case are shown on $m_{\tilde{\nu}_L}$ vs. $\tau_{\tilde{\nu}_L}$ plane. The un-shaded, lightly shaded, and darkly shaded regions are for $a_\nu < 1$, $1 < a_\nu < 10$, and $a_\nu > 10$, respectively. In addition, the contour of $\Omega_{\tilde{\nu}_R}^{(\text{Thermal})} = \Omega_c$ is shown in dotted line. Here, we take $m_{\tilde{\nu}_R} = 100$ GeV, $m_{\tilde{B}} = 1.2m_{\tilde{\nu}_L}$, $\mu_H = 2m_{\tilde{B}}$, $m_h = 115$ GeV, and $\tan\beta = 30$.

$m_{\tilde{\nu}_L} \lesssim 10$ TeV (for $m_{\tilde{\nu}_R} = 100$ GeV). On the contrary, $\Omega_{\tilde{\nu}_R}^{(\text{Thermal})}$ can be as large as Ω_c ; in the figure, we plot the contour of $\Omega_{\tilde{\nu}_R}^{(\text{Thermal})} = \Omega_c$. Here, the a_ν -parameter is determined for given values of $m_{\tilde{\nu}_L}$ and $\tau_{\tilde{\nu}_L}$, while the MSSM parameters are taken to be $m_{\tilde{B}} = 1.2m_{\tilde{\nu}_L}$, and $\mu_H = 2m_{\tilde{B}}$. One can see that, when $m_{\tilde{\nu}_L} \gtrsim 160$ GeV, $\Omega_{\tilde{\nu}_R}^{(\text{Thermal})} = \Omega_c$ can be realized with $a_\nu \lesssim 10$ (which is marginally consistent with the naive order-of-estimate of the a_ν -parameter in gravity-mediated SUSY breaking scenario). Notice that, even with $a_\nu \sim 1$ (or smaller), $\Omega_{\tilde{\nu}_R}^{(\text{Thermal})}$ can be large enough if a larger value of y_ν is adopted or if $\tilde{\nu}_R$ is produced by the decay of some exotic particles.

Next, we consider the $\tilde{\tau}$ -NLSP case. In this case, because the NLSP is charged, it may form a bound state with ${}^4\text{He}$ during the BBN epoch and change the reaction rate [28]. (Such an effect is called $\tilde{\tau}$ -catalyzed effect.) Consequently, ${}^6\text{Li}$ abundance may be significantly enhanced if the lifetime of $\tilde{\tau}$ is longer than $\sim 10^3$ sec. Here, the light-element abundances are calculated by including the $\tilde{\tau}$ -catalyzed effect. Assuming that $\tilde{\tau}$ is almost right-handed, we approximate the primordial abundance as [27]:

$$Y_{\tilde{\tau}} \simeq 7 \times 10^{-14} \times \left(\frac{m_{\tilde{\tau}}}{100 \text{ GeV}} \right), \quad (19)$$

and calculate the light-element abundance. The numerical result is shown in Fig. 3. As in the $\tilde{\nu}_L$ -NLSP case, the parameter space $\tau_{\tilde{\tau}} \gtrsim 10^2$ sec (with $\tau_{\tilde{\tau}}$ being the lifetime of $\tilde{\tau}$) is excluded. In addition, the ${}^4\text{He}$ is overproduced due to $p \leftrightarrow n$ conversion process when

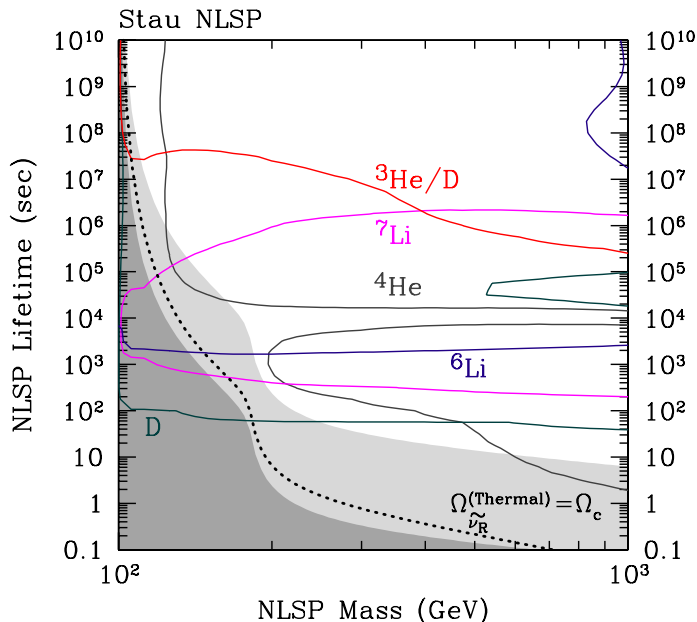


Figure 3: BBN constraints on the $\tilde{\tau}$ -NLSP case are shown on $m_{\tilde{\tau}}$ vs. $\tau_{\tilde{\tau}}$ plane. The un-shaded, lightly shaded, and heavily shaded regions are for $a_\nu < 1$, $1 < a_\nu < 10$, and $a_\nu > 10$, respectively. In addition, the contour of $\Omega_{\tilde{\nu}_R}^{(\text{Thermal})} = \Omega_c$ is shown in dotted line. Here, we take $m_{\tilde{\nu}_R} = 100$ GeV, $m_{\tilde{B}} = 1.2m_{\tilde{\tau}}$, $m_{\tilde{\nu}_L} = 1.2m_{\tilde{\tau}}$, $\mu_H = 2m_{\tilde{B}}$, $m_h = 115$ GeV, $\tan \beta = 30$, and $\sin \theta_{\tilde{\tau}} = 0.3$.

$m_{\tilde{\tau}} \gtrsim 500$ GeV and $\tau_{\tilde{\tau}} \sim 10$ sec. The ^4He constraint becomes more stringent than the $\tilde{\nu}_L$ -NLSP case because the yield variable used in the $\tilde{\tau}$ -NLSP case is larger. We also show the line which satisfies $\Omega_{\tilde{\nu}_R}^{(\text{Thermal})} = \Omega_c$, taking $m_{\tilde{B}} = 1.2m_{\tilde{\tau}}$, $m_{\tilde{\nu}_L} = 1.2m_{\tilde{\tau}}$, $\mu_H = 2m_{\tilde{B}}$, and $\sin \theta_{\tilde{\tau}} = 0.3$. As one can see, the lifetime becomes longer for a given value of a_ν compared to the case of $\tilde{\nu}_L$ -NLSP; this is because we have taken a small value of $\theta_{\tilde{\tau}}$. Even in this case, we can see that $\Omega_{\tilde{\nu}_R}^{(\text{Thermal})} = \Omega_c$ can be realized with $a_\nu \lesssim 10$ in the parameter region consistent with all the BBN constraints.

Finally we comment on the implication of the $\tilde{\nu}_R$ -LSP scenario on the so-called ^7Li problem. As we have mentioned, the standard BBN is excluded at more than $4\text{-}\sigma$ level if we take the face value of the observational constraints on the ^7Li abundance; the theoretical prediction of the ^7Li abundance becomes significantly larger than the observed value. Even though the ^7Li problem does not exist if a significant depletion of ^7Li occurs in stars, the degree of the depletion has not yet been accurately understood. If one adopts models with small depletion, the astrophysical or particle-physics solution to the ^7Li problem is required. It is notable that the ^7Li abundance can be reduced if a long-lived particle decays into hadrons during the BBN epoch [29, 30]. Thus, in the present case, the decay of the NLSP during the BBN may be a solution to the ^7Li problem. In the following, we will see that the ^7Li problem may be solved if \tilde{B} is the NLSP. (For the cases of $\tilde{\nu}_L$ - and $\tilde{\tau}$ -NLSP, the ^7Li problem is hardly solved because the parameter region with the lifetime longer than $\sim 10^2$ sec is (almost) excluded, as shown in Figs. 2 and 3.)

To study the ${}^7\text{Li}$ problem in the present framework, we neglect the systematic error (i.e., +0.35 dex) in the observational constraint on ${}^7\text{Li}$ abundance. In addition, because the allowed parameter region is sensitive to the observational constraint on ${}^7\text{Li}$, we consider two different observational constraints on ${}^7\text{Li}$ abundance:

$$\text{Low } {}^7\text{Li} : \log_{10}(n_{{}^7\text{Li}}/n_{\text{H}})_p = -9.90 \pm 0.09 \text{ [22]}, \quad (20)$$

$$\text{High } {}^7\text{Li} : \log_{10}(n_{{}^7\text{Li}}/n_{\text{H}})_p = -9.63 \pm 0.06 \text{ [26]}. \quad (21)$$

Notice that the low value corresponds to the one given in (17), while the high value is from measurement using different method to estimate temperature of the atmosphere in dwarf halo stars. In addition, because the systematic error in the ${}^6\text{Li}$ to ${}^7\text{Li}$ ratio is correlated to that of ${}^7\text{Li}$, we also remove the systematic error from (16):

$$(n_{{}^6\text{Li}}/n_{{}^7\text{Li}})_p < 0.046 + 0.022. \quad (22)$$

BBN constraints on the Bino-NLSP case are shown in Fig. 4, using the constraints (20) and (22) (upper panel) or (21) and (22) (lower panel). Here, constraints on $(n_{\text{D}}/n_{\text{H}})_p$, Y_p , and $(n_{{}^3\text{He}}/n_{\text{D}})_p$ are unchanged from the previous cases; the D to H ratio given in (13) is called ‘‘Low D’’ because of the reason below. As one can see, if we adopt the high value of the ${}^7\text{Li}$ to H ratio, all the light-element abundances can be consistent with the observational constraints if $10^2 \text{ sec} \lesssim \tau_{\tilde{B}} \lesssim 10^3 \text{ sec}$. On the contrary, with the low value of ${}^7\text{Li}$ abundance, the constraint on the D to H ratio (13) makes it difficult to solve the ${}^7\text{Li}$ problem. However, this conclusion changes if we adopt a slight systematic error in the ${}^7\text{Li}$ abundance, or if a different observational constraint on the D to H ratio is adopted. Indeed, in some literature, a higher value of the D to H ratio (which is the highest value among the data points for six most precise observations [14]) is adopted because D is the most fragile light element and the observed values might reflect the abundance after suffering from some destruction processes:

$$\text{High D} : (n_{\text{D}}/n_{\text{H}})_p = (3.98_{-0.67}^{+0.59}) \times 10^{-5}. \quad (23)$$

(We call this as ‘‘High D.’’) In Fig. 4, we also present the parameter region consistent with the constraint (23) using the dotted line. As one can see, with (23), the ${}^7\text{Li}$ problem can be solved even with the low value of the ${}^7\text{Li}$ to H ratio.

Notice that, in the parameter region where all the light-element abundances become consistent, $\Omega_{\tilde{\nu}_R}^{(\text{Thermal})}$ becomes much smaller than Ω_c if the constraint (20) or (21) is adopted. However, this fact does not imply that the $\tilde{\nu}_R$ -LSP scenario cannot solve the ${}^7\text{Li}$ problem. One possibility is to consider the effects of the decay products of MSSM-LSP after freeze-out; indeed, as shown in the figure, $\Omega_{\tilde{\nu}_R}^{(\text{F.O.})} \simeq \Omega_c$ is realized when $m_{\tilde{B}} \sim 400 \text{ GeV}$ and $\tau_{\tilde{B}} \sim 10^2 \text{ sec}$ with solving the ${}^7\text{Li}$ problem.

Acknowledgments: This work was supported in part by Research Fellowships of the Japan Society for the Promotion of Science for Young Scientists (K.I.), and by the Grant-in-Aid for Scientific Research from the Ministry of Education, Science, Sports, and Culture of Japan, No. 14102004 (M.K.), No. 18071001 (K.K.) and No. 19540255 (T.M.), and also by World Premier International Research Center Initiative, MEXT, Japan (M.K. and T.M.).

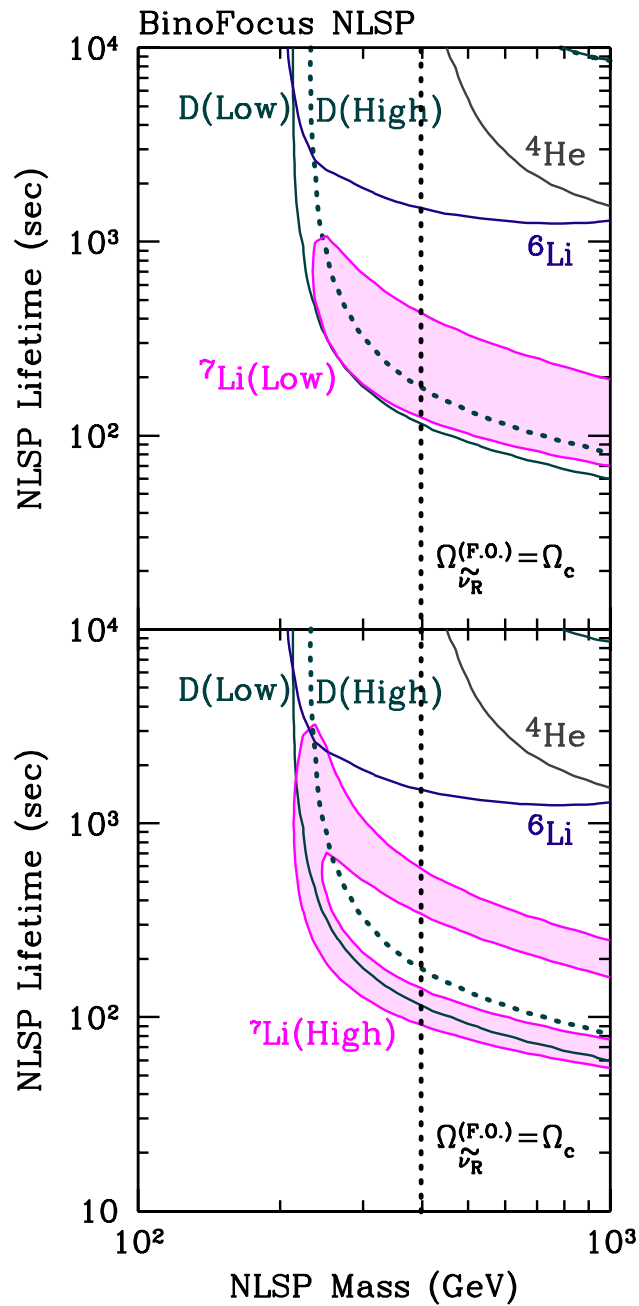


Figure 4: Same as Fig. 1, but with different set of observational constraints. Regions where ⁷Li abundance becomes consistent with the observation are shaded.

References

- [1] G. Hinshaw *et al.* [WMAP Collaboration], *Astrophys. J. Suppl.* **180**, 225 (2009).
- [2] T. Asaka, K. Ishiwata and T. Moroi, *Phys. Rev. D* **73**, 051301 (2006); *Phys. Rev. D* **75**, 065001 (2007).
- [3] L. J. Hall, K. Jedamzik, J. March-Russell and S. M. West, arXiv:0911.1120 [hep-ph].
- [4] T. Moroi, H. Murayama and M. Yamaguchi, *Phys. Lett. B* **303**, 289 (1993).
- [5] J. L. Feng, A. Rajaraman and F. Takayama, *Phys. Rev. Lett.* **91**, 011302 (2003); *Phys. Rev. D* **68**, 063504 (2003).
- [6] K. Ishiwata, S. Matsumoto and T. Moroi, *Phys. Rev. D* **77**, 035004 (2008).
- [7] S. Gopalakrishna, A. de Gouvea and W. Porod, *JCAP* **0605**, 005 (2006); J. March-Russell, C. McCabe, M. McCullough, arXiv:0911.4489 [hep-ph].
- [8] M. H. Ahn *et al.* [K2K Collaboration], *Phys. Rev. D* **74**, 072003 (2006).
- [9] J. L. Feng, S. Su and F. Takayama, *Phys. Rev. D* **70**, 075019 (2004).
- [10] M. Kawasaki, K. Kohri and T. Moroi, *Phys. Lett. B* **625**, 7 (2005); *Phys. Rev. D* **71**, 083502 (2005).
- [11] H. Murayama, I. Watanabe and K. Hagiwara, “HELAS: HELicity amplitude subroutines for Feynman diagram evaluations,” KEK-91-11.
- [12] T. Sjostrand *et al.*, *Comput. Phys. Commun.* **135**, 238 (2001).
- [13] M. Kawasaki and T. Moroi, *Phys. Lett. B* **346**, 27 (1995); T. Kanzaki, M. Kawasaki, K. Kohri and T. Moroi, *Phys. Rev. D* **76**, 105017 (2007).
- [14] J. M. O’Meara *et al.*, *Astrophys. J.* **649**, L61 (2006).
- [15] C. Amsler *et al.* [Particle Data Group], *Phys. Lett. B* **667**, 1 (2008).
- [16] Y. I. Izotov, T. X. Thuan and G. Stasinska, arXiv:astro-ph/0702072.
- [17] M. Fukugita and M. Kawasaki, *Astrophys. J.* **646**, 691 (2006).
- [18] J. Geiss and G. Gloeckler, *Space Science Reviews* **106**, 3 (2003).
- [19] M. Asplund *et al.*, *Astrophys. J.* **644**, 229 (2006).
- [20] J. Hisano *et al.*, *Phys. Rev. D* **79**, 083522 (2009).
- [21] A. E. G. Perez *et al.*, arXiv:0909.5163 [astro-ph.SR].

- [22] P. Bonifacio *et al.*, arXiv:astro-ph/0610245.
- [23] M. H. Pinsonneault, T. P. Walker, G. Steigman and V. K. Narayanan, *Astrophys. J.* **527**, 180 (2002); M. H. Pinsonneault, G. Steigman, T. P. Walker and V. K. Narayanan, *Astrophys. J.* **574**, 398 (2002).
- [24] A. J. Korn *et al.*, *Nature* **442**, 657 (2006).
- [25] R. H. Cyburt, B. D. Fields and K. A. Olive, *JCAP* **0811**, 012 (2008); R. H. Cyburt and B. Davids, *Phys. Rev. C* **78**, 064614 (2008).
- [26] J. Melendez and I. Ramirez, *Astrophys. J.* **615**, L33 (2004).
- [27] M. Fujii, M. Ibe and T. Yanagida, *Phys. Lett. B* **579**, 6 (2004).
- [28] M. Pospelov, *Phys. Rev. Lett.* **98**, 231301 (2007).
- [29] K. Jedamzik, *Phys. Rev. D* **70**, 063524 (2004).
- [30] D. Cumberbatch *et al.*, *Phys. Rev. D* **76**, 123005 (2007).